



Review

Textural and thermal conductivity properties of a low density mesoporous silica material



Ebenezer Twumasi Afriyie*, Peyman Karami, Peter Norberg, Kjartan Gudmundsson

Department of Civil and Architectural Engineering, KTH, Sweden

ARTICLE INFO

Article history:

Received 22 June 2013

Received in revised form

31 December 2013

Accepted 6 February 2014

Keywords:

Low density

Nanopore size

Porosity

Thermal conductivity

ABSTRACT

In this study, the pore structure, tapped density and thermal conductivity properties of a new type of nanoporous silica material have been studied. We have applied nitrogen physisorption, high resolution scanning microscopy and Transient Plane Source thermal conductivity measurements to investigate these properties. The new mesoporous silica SNP have large BET surface area, $400\text{--}439 \text{ m}^2 \text{ g}^{-1}$ and possess high porosity in the range of 95–97%. The results further show pore diameter centred at 43 nm or 47 nm for the two materials studied. Tapped densities as low as 0.077 g/cm^3 have so far been obtained and the thermal conductivity of these materials has been measured to 0.0284 and $0.0294 \text{ W} (\text{m K})^{-1}$ at room temperature and atmospheric pressure. The effects of tapped density, pore size diameter and particle morphology on thermal conductivity are discussed.

© 2014 Elsevier B.V. All rights reserved.

Contents

1. Introduction	210
2. Experimental	211
2.1. Materials	211
2.2. Preparation of nanoporous silica	212
2.3. Materials characterization	212
2.4. Thermal conductivity measurements	212
3. Results and discussion	212
3.1. Textural properties	212
3.2. Thermal conductivity	212
4. Conclusion	214
Acknowledgements	214
References	214

1. Introduction

Nanoporous materials offer some of the lowest reported thermal conductivity values owing to their unique properties such as low density, large surface area and high porosity [1,2]. Increasing

evidence of the inadequate nature of our major energy resources and large cost as well as consumption associated with environmental concerns, mandate utilization of advanced thermal insulation. One such insulation is vacuum insulation panels (VIP) [3,5] which are made of an evacuated open porous material such as fumed or precipitated silica and also glass fibres, placed inside a multilayer envelope and makes use of vacuum to suppress the gaseous heat transfer to zero. Because of its exceptional insulation properties, also silica aerogel has been suggested as a candidate material as VIP core material. Its possible utilization comes about as a result of their high porosity, large surface area, small pores as well as low density and low thermal conductivity. Aerogel for example, may have a large surface area ($\sim 1600 \text{ m}^2 \text{ g}^{-1}$) and pores in the range between 5 and 100 nm depending on the synthesis method and the

Abbreviations: NLDFT, nonlocal density functional theory; p/p_0 , relative pressure; PSD, pore size distribution; S_{BET} , specific surface area obtained via Brunauer–Emmett–Teller-equation; SNP, Silica NanoPorous material; V_{tot} , total pore volume; ρ_a , actual density obtained by compressed powder; ρ_b , tapped density obtained by mechanical tapping.

* Corresponding author at: University of Gävle, Sweden. Tel.: +46 709748751; fax: +46 26648181.

E-mail address: twumasi@kth.se (E.T. Afriyie).

silica source used [2]. These pores occupy about 80–99.8% of their total bulk volume. As a result of these small pores and the high porosity, aerogels exhibit extraordinary physical, thermal, acoustical and optical properties. A bulk density as low as 0.003 g/cm^3 has been reported while for typical application aerogel with values of about $0.07\text{--}0.15\text{ g/cm}^3$ is used [2,3]. A low thermal conductivity of $0.017\text{--}0.021\text{ W (m K)}^{-1}$ at ambient pressure has been established [2,3]. Fumed silica on the other hand has porosity greater than 90% and a tapped density in the range of $0.06\text{--}0.22\text{ g/cm}^3$ [5,6]. The material also has a specific surface area in the range of $100\text{--}400\text{ m}^2\text{ g}^{-1}$ which varies with the particle size and a maximum pore size value of about 300 nm has been reported [4]. A thermal conductivity of about 0.02 W (m K)^{-1} at atmospheric pressure has been proven [5,6]. Despite their obvious technical advantages, their utilization as thermal insulation media in building industry is limited due to their high market price [2–6]. This high cost of aerogel and fumed silica does not arise basically from starting materials but generally from the manufacturing process [2,7]. The fumed silica production is more energy intensive than the silica obtained by sol gel or precipitation method [7,8]. Classical silica aerogels have been produced by drying wet gels under supercritical conditions [2]. However, large-scale production is limited, because of the high cost and hazardous nature of the process [9]. Several attempts have been made to develop alternative method for large-scale production and one success is ambient pressure drying process [2,9]. By this technique, the capillary forces are reduced through the formation of new siloxane bonds on wet gel and provide a spring-back effect to reduced networks shrinkage during drying [2,9]. However, this method suffers from the higher material costs and the drying process which involves the use of hazardous solvents for tedious solvent exchange and surface modification, which is harmful to humans and the environment [9]. In an attempt to eliminate or minimize these problems, Cabot and NanoPore have developed two new ambient pressure processes [10]. Although ambient pressure aerogel production is ongoing at Cabot and NanoPore, still at relatively high costs in terms of insulating performance basis as compared to other insulation. On the other hand, the preparation of different nanoporous silicas with promising thermal properties has been reported [11,12]. Although their work seems very interesting, the preparation procedures is time-consuming and required the used of large amount of hazardous solvents.

VIPs made with nanoporous core material have been shown to have superior performance over those made of microporous materials [3,5,13,14]. However, the high cost of nanoporous materials is one of the major reasons behind the high cost of VIPs and its limited utilization in building industry. In order to overcome this cost barrier for the mass application of VIPs in the building industry, alternative low-cost nanoporous core material needs to be developed. The nanoporous material must achieve not only the thermal performance which provides value to the customer but also can be obtained by a simplified production route that is cost effective and environmental friendly. To avoid high costs associated with siloxane silica source and use of hazardous solvents as well as tedious synthesis route, the present work has been aimed at the use of sodium silicate and glycerol as template to synthesis low density nanoporous material.

The classical method known for measurement of thermal conductivity is a guarded hot-plate. This consists of sandwiching a material between two plates that are held at different constant temperatures, permitting the temperature distribution across the material to go to steady state and then measuring the resulting heat flux through the material. The gain of this method is the accuracy of the results. The drawbacks include the need for large dimensions of the testing sample, the unidentified contact resistances between the material and the two plates, and the long period of time it takes to run each test. Much faster methods are transient methods. It

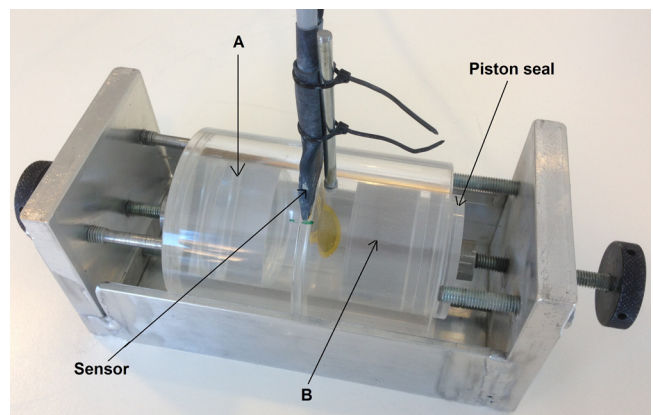


Fig. 1. Test setup for performing the transient thermal measurement on SNPs powders.

is basically a flat coil of thin wire with known temperature resistance. The coil is also sandwiched between two test sample material (Fig. 1) and a current is run across the wire and its temperature changes at a rate that depends on the thermal conductivity of the surrounding material. The coil acts both as a heat source for increasing the temperature of the sample and a “resistance thermometer” for recording the time dependent temperature increase. The short time interval to run the measurement makes it possible to neglect the end effects of the finite size of metal strip and the temperature distribution around and in the coil is identical to that of an infinitely long plane heat source. Further the method can measure much smaller sample sizes and of any shapes. Both the thermal conductivity and diffusivity can however be acquired simultaneously with the transient methods while two measurements are generally required when using stationary method. One drawback of TPS measurement has been the use of two sample pieces that each needs to have one entirely planar side. This makes it difficult to achieve for some materials especially powders or granules. This work addresses that drawback.

A test setup involving a sensor holder has been developed which enables the powder to be compacted and enhance thermal contact between the powder and the sensor (see Fig. 1.). Again different thermal conductivity can be obtained at different densities by compressing the powder to different volumes. The Transient Plane Source (TPS) method has been demonstrated in a study by Gustafsson [15] and even an improvement of the technique in different reports [16–18]. The TPS measurement technique is described in detail by Log and Gustafsson [19], while the theoretical considerations have been summarized by He [20]. In addition, Von Herzen et al. [21] applied needle probes as heat source for creating transient increase in temperature inside test samples. Much works has also been done with emphasis on developing the accuracy of TPS technique and the method has been studied and used by numerous authors [22–28]. In this work, commercially available Transient Plane Source (TPS) (ISO 22007-2) equipment was employed to measure the thermal conductivity of newly developed silica powders and commercial aerogel [14] as reference material.

2. Experimental

2.1. Materials

The chemicals used for the synthesis of mesoporous silicas were sodium silicate ($\text{SiO}_2:\text{Na}_2\text{O} = 3.35:1$), sodium hydroxide (NaOH), sodium chloride (NaCl), glycerol ($\text{CH}_2\text{OHCHOHCH}_2\text{OH}$), oxalic acid ($\text{HO}_2\text{CCO}_2\text{H}$) and sulphuric acid (H_2SO_4). The sodium silicate was

purchased from Sibelco, Göteborg, Sweden, and the salt originated from retailers of agricultural chemicals. The rest of the chemicals were purchased from Sigma–Aldrich, Sweden. Ordinary tap water was used for the preparation.

2.2. Preparation of nanoporous silica

In preparing the nanoporous silica, a sodium chloride solution was added to sodium silicate solution of pH in the range of 8–9 and with 35% glycerol. The addition of salt solution to the silica solution was done under rapid stirring in the presence of a base catalyst (NaOH) at room temperature. Sulphuric acid and oxalic acid were used to control the pH of the silica solution. The resultant reaction mixture contains 0.7 mol ratio of acid to base and salt to silica mole ratio of 0.26. A 3 M H₂SO₄ or oxalic acid solution was added drop-wise to the reaction mixture under continuous stirring for about 10 min, until the pH became about 7. The semi-transparent gel was aged for 4 h and washed with a defined amount of water until the gel was free from sodium and sulphate ions. After final washing the gel was vacuum filtered and a laboratory-scale spray dryer (BÜCHI mini spray dryer B-290) was employed to obtain dried silica powder. The Silica NanoPorous (SNP) powders were designated by abbreviations indicating the acids, sulphuric acid (SA) and oxalic acid (OA), such as SNP-SA and SNP-OA.

2.3. Materials characterization

The textural properties of the mesopore silicas were studied by nitrogen adsorption at 77 K using a Micromeritics TriStar 3. Before measurement the materials were degassed under nitrogen condition for 3 hours at 250 °C. The specific surface area and pore size were evaluated by Brunauer–Emmet–Teller (BET) and density functional theory (DFT) methods, respectively. Multipoint BET surface areas (S_{BET}) were obtained for all samples with a minimum of 6 points and a correlation coefficient of 0.9999. This was evaluated using nitrogen adsorption isotherm data in the relative pressure (p/p_0) range from 0.05 to 0.3. The total pore volume (V_{tot}) was estimated on the basis of the amount adsorbed at $p/p_0 \approx 0.99$.

Pore size distribution (PSD) curves were derived assuming Carbon Slit Pores by NLDFT model and slit pore geometry as these model fit the samples. The selected model is applied over the entire range of the adsorption branch of the isotherm and is not restricted to a limited range of relative pressure or pore size. PSD is calculated by fitting to a theoretical set of adsorption isotherms, evaluated for different pore sizes and shapes in the analysis software, to the experimental N2 adsorption isotherm. The best fitting model to the experimental isotherm then gives the PSD.

The morphology was observed by Carl Zeiss scanning electron microscopy.

2.4. Thermal conductivity measurements

Before the measurement of thermal conductivity, the powder materials were dried overnight in a stationary dryer at 105 °C to remove moisture. Reference commercial silica aerogel material was received in granular form and was pulverized into powder herein refers to as X and dried likewise at 105 °C. In actual measurement (Fig. 1) first a piston-shaped seal is placed at the bottom of a hollow cylinder (Part B) and is filled with known amount of powder to the top edge, then the sensor with radius 6.403 mm is placed on top of the powder and tightened to Part B holder. Second, the other part of the hollow cylinder (Part A) is placed on Part B, and is also filled with an equal amount of powder.

This is followed by another piston-shaped seal placed in the hollow cylinder. The two parts A and B with a sensor in between are tightened. The initial volume on each part is measured and from

that an initial density is calculated. The volume change as compressing the powder is measured and then subsequent densities are calculated. The densities obtained by compressed powder will herein refer to as actual density (ρ_a). The thermal conductivity was measured at 22 °C with an output power of 0.005 W and a measurement time of 160 s. A time lapse of 20 min between each reading was employed.

The tapped density (ρ_b) of the mesoporous silica powders was measured by placing a known amount of the powder into a graduated cylinder, which was tapped 500 times using Jolting Volumeter STAV II (J. Engelmann AG, Germany). The volume occupied by the powder was then read and the density calculated based on the mass to volume ratio. The porosity of the samples was calculated by the relation:

$$\text{Porosity}(\%) \left[1 - \frac{\rho_b}{\rho_s} \right] \times 100 \quad (1)$$

where ρ_b and ρ_s are the tapped and skeletal densities of the SNP, respectively. The skeletal density ρ_s of pure silica 2.5 g/cm³ was used.

3. Results and discussion

3.1. Textural properties

Fig. 2 shows the physisorption isotherms and the corresponding physicochemical parameters are summarized in Table 1. The isotherms are of type IV with a type H4 hysteresis loop based on IUPAC classification [29]. The shape of the hysteresis loop (type H4) can be attributed to the presence of narrow slit-like pores [29]. The SNP-SA exhibit a high surface area of 439 m² g⁻¹, and the maximum pore size peak centred at about 47 nm as shown in Fig. 2b. The S_{BET} and pore size of the SNP-OA were slightly lowered with the variation of the acid type. This similar pore size was obtained by [30] when glycerol was used as drying control chemical additives in aerogel preparation [30]. The variation of acid type from oxalic acid to sulphuric acid influence the tapped density and the porosity. The tapped density and porosity of 0.122 g/cm³ and 95.1% were observed for SNP-OA whereas for SNP-SA the density decreases to 0.077 g/cm³ and the porosity increases to 96.9% respectively. Such high surface area and homogeneity of pore size can be attributed to glycerol–silica clusters via formation of hydrogen bonds. The glycerol thus provides a steric shielding around the colloidal particles, preventing rapid precipitation. A delay in precipitation reaction would results in small homogenous particles which provide large surface area. Moreover, the presence of glycerol in the SNP pore system shift the pore size distribution to large mean pore sizes, which reduce the degree of drying stress caused by the surface tension. Thus the SNP-SA with large pore size has a less tapped density as there was less stress or shrinkage during drying. The mean pore sizes of the SNP materials are smaller than the mean free path of air (~70 nm) under ambient conditions, indicating that the SNP's can retard the gaseous heat conduction even under ambient condition in accordance with Knudsen number [3,6]. Fig. 3 shows the SEM images of the SNPs made with different acids and have different tapped densities. The SNP-OA exhibits morphology of spherical and plate-like particles whereas SNP-SA displays only particles of spherical nature. Both morphologies also confirm the porous nature of the powder with relatively uniform pores in the particles (Fig. 3c and d).

3.2. Thermal conductivity

The thermal conductivity for the SNPs under study as a function of the actual density, obtained by TPS is shown in Table 1 and the Fig. 4. The first important result is that the trends observed by both

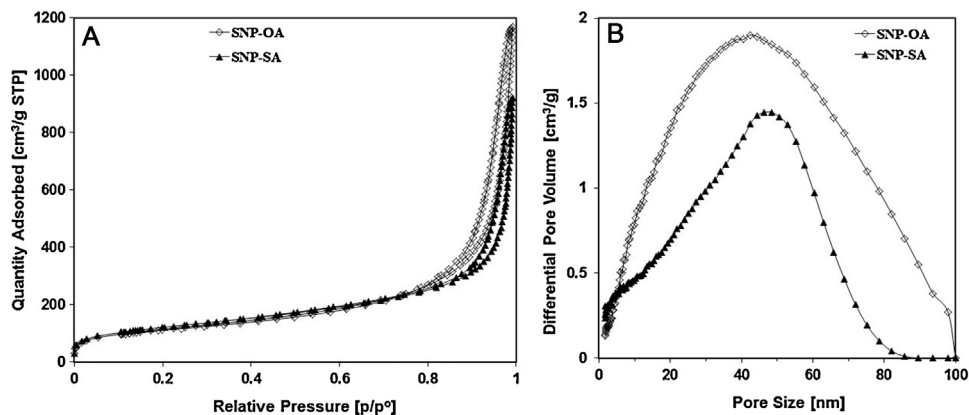


Fig. 2. Nitrogen adsorption–desorption isotherm (A) and (B) pore size distribution of SNP powders. PSD have been determined by NLDFT Carbon slit pores model and slit pore geometry.

Table 1

Physical and thermal conductivity properties of SNP powders and reference material.

Sample ID	S_{BET} ($\text{m}^2 \text{ g}^{-1}$)	PS (nm)	V_{tot} ($\text{cm}^3 \text{ g}^{-1}$)	ρ_b (g/cm^3)	Porosity (%)	λ_{int} ($\text{W} (\text{m K})^{-1}$)	λ_{finl} ($\text{W}(\text{mK})^{-1}$)
X	686	26	3.5	0.085	96.1	0.0265	0.0201
SNP-OA	412	43	1.8	0.122	95.1	0.0284	0.0336
SNP-SA	439	47	1.4	0.077	96.9	0.0314	0.0294

X – pulverized commercial aerogel material, ρ_b – tapped density, SBET – BET specific surface area, V_{tot} – total pore volume, PS – pore size centred on maxima peaks in DFT pore size distribution, λ_{int} – thermal conductivity without compressing the powder, λ_{finl} – thermal conductivity after final compressing.

materials as a function of actual density are very different (Fig. 4). The thermal conductivity of SNP-OA is low ($0.0284 \text{ W} (\text{m K})^{-1}$) at actual density of $0.092 \text{ g}/\text{cm}^3$, and then slightly increases with density. On the contrary, the SNP-SA at $0.064 \text{ g}/\text{cm}^3$ actual density, the thermal conductivity is $0.0314 \text{ W} (\text{m K})^{-1}$ then decreases slightly as the powder is compressed. The best thermal conductivity ($0.0294 \text{ W} (\text{m K})^{-1}$) is then obtained at $0.146 \text{ g}/\text{cm}^3$ actual density at final compressing. The thermal conductivity for commercially available aerogel material (X) has also been mea-

sured at different actual densities. The commercial reference material has already been characterized [14] and thus there is a known thermal conductivity available to compare to the measured results using the TPS method. The reported thermal conductivity value for the commercial material X is $0.018 \text{ W} (\text{m K})^{-1}$ at ambient pressure [14]. Our result was $0.0201 \text{ W} (\text{m K})^{-1}$ at final compressed density at the same pressure. It is worth to note that the thermal conductivity measured for the reference material X by [14] using

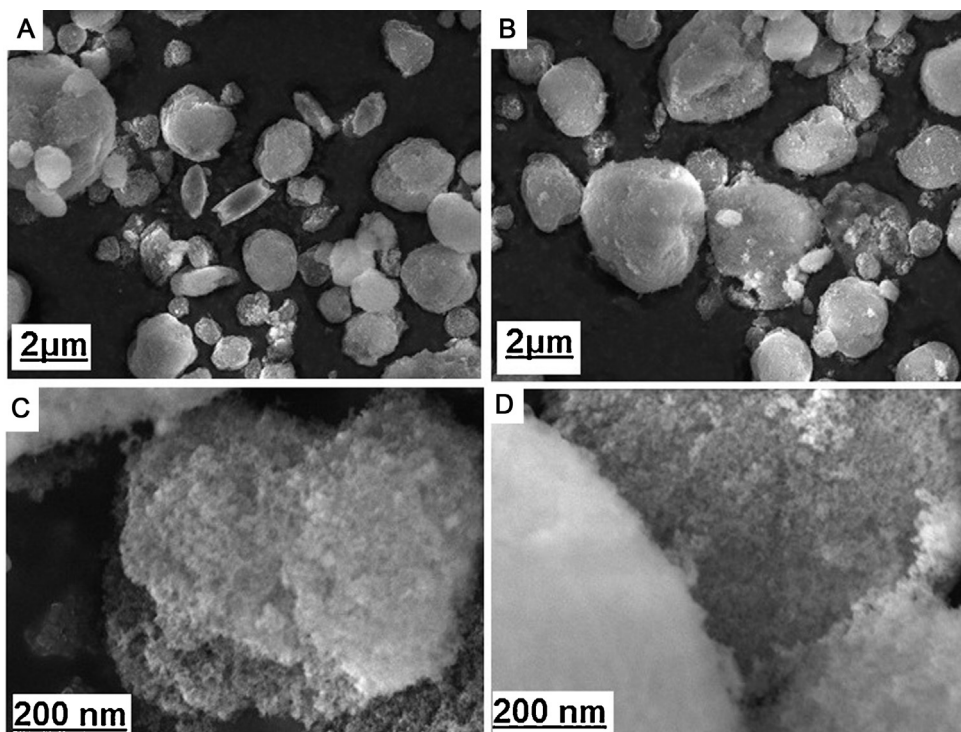


Fig. 3. SEM images of the SNPs made with different acids. (A, C) Oxalic acid and (B, D) sulphuric acid.

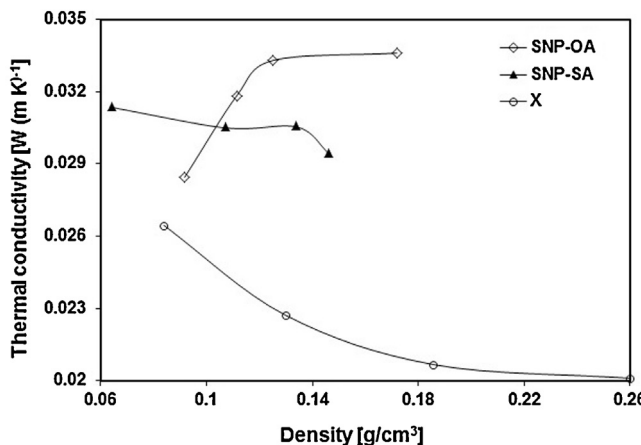


Fig. 4. Total thermal conductivity of SNP powder samples versus their actual densities obtained by compressed powder. Included is commercial material (X) used as reference.

Transient hot-wire method gave a result of $0.0197 \text{ W} (\text{m K})^{-1}$ at ambient pressure.

The foregoing phenomena in SNP powders can be explained as follows. The modelling of the effect of particle packing on total thermal conductivity has been shown by many studies [31–33] and proven that contact areas and the contact resistances have a significant effect on the conductive properties when the particles volume is reduced by external load. Primarily, the theoretical dependence of the thermal conductivity on the external load is influenced merely by a compaction of the powder. Upon compression of the powder, two factors, particle morphology and actual density, were coherently observed to influence the thermal conductivity. Under compression the porosity of the powders will be decrease which influences the grain-to-grain geometric and contact resistance. For SNP-OA powder, upon gradual compressing, the plate and spherical particles (see Fig. 3) may begin to overlap and the gap between the particles will be lowered. The increased contact areas and reduced gap will result in increase in actual density (Fig. 4) and make the system behave like a homogenous material. The temperature gradient and hence heat flux is almost uniformly distributed and consequently promotes rapid solid conduction which reaches the maximum value that represent the dense powder.

In the case of SNP-SA, where the particles are spherical aggregates, the compressing of the powder will lower the pores or gaps between the particles and also increase in actual density; however the tendency of overlapping may be reduced or eliminated (see Fig. 3d). The conductivity of the powder will therefore be determined by the space between the conducting particles which can be consider as a resistor network that retard gas conduction. The rate of solid conduction contribution is also less compared to compacted SNP-OA system as the compacted SNP-SA density is less. The reduction of the gap by compression will therefore results in lowering the total thermal conductivity as seen in SNP-SA thermal conductivity values. The same behaviour as in SNP-SA system was observed for the reference commercial material.

Although the thermal conductivity is higher for our SNP powders than for aerogels and fumed silica in reports [2–6,14], our technique is simple, inexpensive and environmental friendly, and can be used in large-scale thermal insulating applications at low pressures such as VIP [3,5].

4. Conclusion

Mesoporous silicas with low density have been prepared using sodium silicate and glycerol as template. The influence of the

synthesis parameter such as type of acid on the textural and thermal conductivity properties has been observed. The use of glycerol as template resulted in formation of porous silica of homogenous pore structure and high specific surface area. The type of acid used in the synthesis determines the particle morphology, porous structure as well as the tapped density. Thermal conductivity measurements indicate that the lowest thermal conductivity can be obtained at actual density of 0.092 g/cm^3 for SNP obtained by oxalic acid whereas for SNP obtained by sulphuric acid a low thermal conductivity was obtained at actual density of 0.146 g/cm^3 . Thus under compression, the actual density at which the smallest thermal conductivity can be obtained is particle morphology dependent. At higher compression, spherical particles will be more efficient in the reduction of the total thermal conductivity by forming small pore network and reducing gas conduction. Therefore, one should consider the particle morphology in designing low density mesoporous silica for thermal insulation applications. The synthesis method employed here is simple, fast and environmental friendly and resulted in material that is promising for thermal insulation application.

Acknowledgements

Many thanks to Professor Klaus Leifer and Dr. Thomas Thersleff at Department of Engineering Science, Uppsala University, for their assistance with SEM images.

References

- [1] G.Q. Lu, X.S. Zhao, Nanoporous Materials Science and Engineering, Series of Chemical Engineering, Vol. 4, Imperial College Press, London, UK, 2004, pp. 1–12.
- [2] N. Hüsing, U. Schubert, Aerogels-airy materials: chemistry, structure, and properties, *Angewandte Chemie International Edition* 37 (1998) 22–45.
- [3] R. Baetens, B.P. Jelle, J.V. Thue, M.J. Tempierik, S. Grynning, S. Uvsløkk, A. Gustavsen, Vacuum insulation panels for building application: a review and beyond, *Energy Buildings* 42 (2010) 147–172.
- [4] V.M. Gun'ko, et al., Morphology and surface properties of fumed silicas, *Journal of Colloid and Interface Science* 289 (2005) 427–445.
- [5] M. Alam, H. Singh, M.C. Limbachiyia, Vacuum Insulation Panels (VIPs) for building construction industry – a review of the contemporary developments and future directions, *Applied Energy* 88 (2011) 3592–3602.
- [6] D. Quenard, H. Salle, Micro-nano porous materials for high performance thermal insulation, in: Proceedings of 2nd International Symposium on Nanotechnology in Construction conference, Bilbao-013-16, November, 2005.
- [7] R.K. Iler, The Chemistry of Silica Chemistry, Wiley-Interscience Publication, 1972, ISBN 0-471-02404-X, pp. 565–567.
- [8] S. Vermury, S.E. Pratsinis, Charging and Coagulation during flame synthesis of silica, *Journal of Aerosol Science* 27 (6) (1996) 951–966.
- [9] D.M. Smith, A. Maskara, U. Boes, Aerogel-based thermal insulation, *Journal of Non-crystalline Solids* 225 (1998) 254–259.
- [10] S. Wallace, et al., US patent applications, 1997.
- [11] B.P. Jelle, et al., Thermal Insulation Materials, international patent application PCT/NO2012/050045, 2012.
- [12] L.F. Su, L. Miao, S. Tanemura, G. Xu, Low-cost and fast synthesis of nanoporous silica cryogels for thermal insulation applications, *Science and Technology of Advanced Materials* 13 (2012) 035003.
- [13] R. Caps, H. Beyrichen, D. Kraus, S. Weismann, Quality control of vacuum insulation panels: methods of measuring gas pressure, *Vacuum* 82 (2008) 691–699.
- [14] E. Cohen, Thermal Properties of Advanced Aerogel Insulation, Massachusetts Institute of Technology (Master Thesis), 2011.
- [15] S.E. Gustafsson, Zeitschrift für Naturforschung A. Teil, Department of Physics, Chalmers University of Technology, S41296, Gothenburg, Sweden, 22a (1967) 1005.
- [16] S.E. Gustafsson, E. Karawacki, M.N. Khan, Transient hot-strip method for simultaneously measuring thermal conductivity and thermal diffusivity of solids and fluids, *Journal of Physics D: Applied Physics* 12 (1979) 1411–1421.
- [17] S.E. Gustafsson, Device for measuring thermal properties of a test substance – the transient plane source (TPS) method, U.S. Patent # 5,044,767 (1991).
- [18] S.E. Gustafsson, Transient plane source techniques for thermal conductivity and thermal diffusivity measurements of solid materials, *Review of Scientific Instruments* 62 (1991) 797–804.
- [19] T. Log, S.E. Gustafsson, Transient plane source (TPS) technique for measuring thermal transport properties of building materials, *Fire Materials* 19 (1995) 43–49.
- [20] Y. He, Rapid thermal conductivity measurement with a hot disk sensor, Part I. Theoretical considerations, *Thermochimica Acta* 436 (2005) 122–129.

- [21] R. Von Herzen, A.E. Maxwell, The measurement of thermal conductivity of deep-sea sediments by a needle-probe method, *Journal of Geophysical Research* 64 (10) (1959) 1557–1563.
- [22] M. Gustavsson, E. Karawacki, S.E. Gustafsson, Thermal conductivity, thermal diffusivity, and specific heat of thin samples from transient measurements with hot disk sensors, *Review of Scientific Instruments* 65 (12) (1994).
- [23] V. Bohac, M.K. Gustavsson, L. Kubicar, S.E. Gustafsson, Parameter estimations for measurements of thermal transport properties with the hot disk thermal constants analyser, *Review of Scientific Instruments* 71 (2000) 2452–2455.
- [24] M. Gustavsson, S.E. Gustafsson, *Thermal Conductivity*, vol. 27, DEStech Pubs. Inc., Lancaster, PA, 2003, pp. 338–346.
- [25] Y. Jannot, Z. Acem, A quadrupolar complete model of the hot disc, *Measurement Science and Technology* 18 (2007) 1229–1234.
- [26] M. Gustavsson, S.E. Gustafsson, Thermal conductivity as an indicator of fat content in milk, *Thermochimica Acta* 442 (2006) 1–5.
- [27] S. Malinaric, Parameter estimation in dynamic plane source method, *Measurement Science and Technology* 15 (2004) 807–813.
- [28] S.A. Al-Ajlan, Measurements of thermal properties of insulation materials by using transient plane source technique, *Applied Thermal Engineering* 26 (2006) 2184–2191.
- [29] K.S.W. Sing, D.H. Everett, R.A.W. Haul, L. Moscou, R.A. Pierotti, J. Rouquerol, T. Siemieniewska, Reporting physisorption data for gas/solid systems with special reference to the determination of surface area and porosity, *Pure and Applied Chemistry* 57 (4) (1985) 603–619.
- [30] A.V. Rao, M.M. Kulkarni, Effect of glycerol on physical properties of hydrophobic silica aerogels, *Materials Chemistry and Physics* 77 (2002) 819–825.
- [31] W. Evans, R. Prasher, J. Fish, P. Meakin, P. Phelan, P. Keblinski, Effect of aggregation and interfacial thermal resistance on thermal conductivity of nanocomposites and colloidal nanofluids, *International Journal of Heat and Mass Transfer* 51 (2008) 1431–1438.
- [32] Y.B. Yi, The role of interparticle contact in conductive properties of random particulate materials, *Acta Materialia* 56 (2008) 2810–2818.
- [33] C. Argento, D. Bouvard, Modeling the effective thermal conductivity of random packing of spheres through densification, *International Journal of Heat and Mass Transfer* 39 (7) (1996) 1343–1350.